Neural Networks Detect Inter-Turn Short Circuit Faults Using Inverter Switching Statistics for a Closed-Loop Controlled Motor Drive

Mustafa Umit Oner, İlker Şahin, *Member, IEEE,* and Ozan Keysan, *Member, IEEE,*

***Abstract*—Early detection of an inter-turn short circuit fault (ISCF) can reduce repair costs and downtime of an electrical machine. In an induction machine (IM) driven by an inverter with a model predictive control (MPC) algorithm, the controller outputs are influenced by a fault due to the fault-controller interaction. Based on this observation, this study developed neural network models using inverter switching statistics to detect the ISCF of an IM. The method was non-invasive, and it did not require any additional sensors. In the fault detection task, an area under receiver operating characteristics curve value of 0.9950 (95% Confidence IntervaI: 0.9949 - 0.9951) was obtained. At the rated operating conditions, the neural network model detected and located an ISCF of 2-turns (out of 104 turns per phase) under 0.1 seconds, a speedup of more than two times compared to the thresholding-based method. Moreover, we published the switching vector data collected at various load torque and shaft speed values for healthy and faulty states of the IM, becoming the first publicly available ISCF detection dataset. Together with the dataset, we provided performance baselines for three main neural network architectures, namely, multi-layer perceptron, convolutional neural network, and recurrent neural network.**

***Index Terms*—Condition monitoring, fault diagnosis, induction motor, machine learning, motor drives, multi-layer perceptron, neural networks, model predictive control.**

I. Introduction

OWING to its value and significance, fault diagnosis of electrical machines has been a focus of intensive research, as reflected by a plethora of publications over the past years [1]–[4]. The early detection of an incipient fault can enable repair cost and downtime reduction benefits. Furthermore, provided that the machine is fault-tolerant by design and proper identification of the inflicting fault is made, the continuum of operation with a reduced rating is also possible.

Several fault detection methods that address induction motors (IM) have been reported [5]–[7] as the IM is the most

Manuscript received Month xx, 2xxx; revised Month xx, xxxx; accepted Month x, xxxx. This work was supported in part by the xxx Department of xxx under Grant (sponsor and financial support acknowledgment goes here).

Mustafa Umit Oner is with the Artificial Intelligence Engineering Department, Bahcesehir University, Istanbul 34349, Turkiye (e-mail: mustafaumit.oner@eng.bau.edu.tr).

İlker Şahin is with ASELSAN Inc, Ankara 06200, Turkiye (e-mail: ilkersahin@aselsan.com.tr).

Ozan Keysan is with the Electrical and Electronics Engineering Department, Middle East Technical University, Ankara 06800, Turkiye (e-mail: keysan@metu.edu.tr).

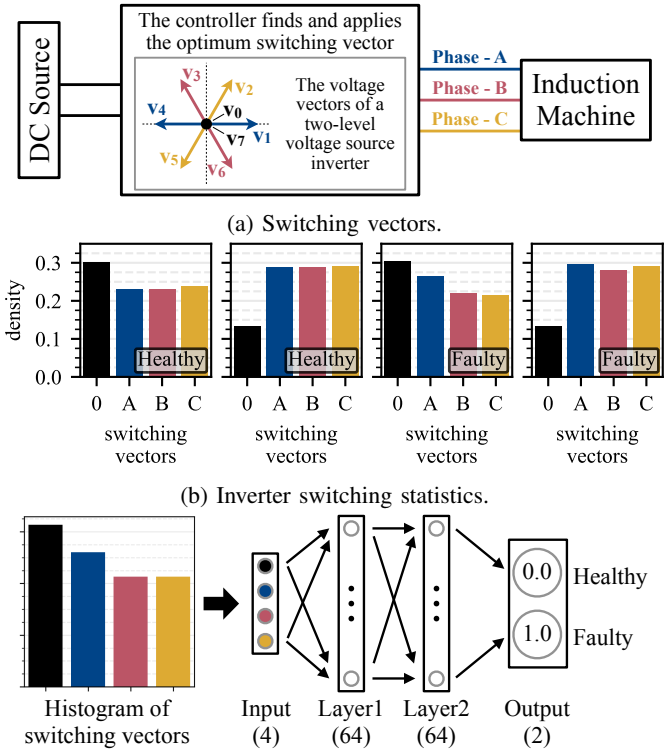

Fig. 1: **Inverter switching statistics and neural network model. (a)** The voltage vectors of a two-level voltage source inverter. The controller finds the optimum voltage vector in view of the control outcomes, and applies it at the next switching instant. **(b)** Histograms of switching vectors over a period for a healthy machine and a machine with inter-turn short circuit fault are given. While aggregated 0-vectors is represented as 0, aggregated active vectors are represented as A, B and C. **(c)** The neural network model is a multi-layer perceptron consisting of an input layer (with 4 nodes), two hidden layers (Layer1 and Layer2 - each with 64 nodes) and an output layer (with 2 nodes). The model takes a histogram of switching vectors at the input and predicts whether the machine is healthy or faulty at the output.

commonly used AC machine type due to its low cost and ruggedness. It is estimated that the stator faults constitute 21% of all the faults [8]. Stator faults usually start as inter-turn short circuit faults (ISCF) [9] and quickly develop further into complete phase-to-phase or phase-to-ground faults, which implies the total malfunctioning of the machine. Depending on the machine and the fault's structure, the time between ISCF occurrence and the total loss of insulation is in the order of seconds [10]. Therefore, a swift and effective identification of an incipient ISCF is crucial.

An important distinction regarding the fault detection studies is the control method assumed for the motor. The motor can be line-fed (uncontrolled, open-loop) or closed-loop controlled via an inverter. There exists a complex interaction between the fault and the controller [11]–[14]. The controller inherently tries to negate the fault's effect. The bandwidth of the controller, hence the current regulating performance, emerges as an important parameter influencing fault-controller interaction [13], [14]. It is shown in [15] that an IM drive implemented with finite control set model predictive control (FCS-MPC) continues to exhibit perfectly balanced phase currents under an ISCF of 3-turns (out of 104 turns per phase). However, a significant unbalance is observed for the line-fed operation under the same fault condition. This example implies that most fault detection methods developed considering line-fed machines (such as motor current signature analysis) would be less effective (if not totally useless) for a high-performance control case. Therefore, it is essential to develop a fault detection method in conjunction with the main control algorithm.

A majority of closed-loop studies in the literature considers field oriented control (FOC) and searches for certain frequency components in phase currents or dq-axes voltages to identify an ISCF [12], [16]–[22]. Similar frequency domain approaches have been presented for direct torque control (DTC) in [23]–[25]. Observing the changes in motor impedance due to an ISCF can also be addressed as a tool for fault diagnosis [11], [26]–[28]. The changes in negative sequence impedance [11], high frequency impedance [26], increased PWM ripple [27], and current estimation error [28] are utilized for diagnostic purposes. Other examples include utilization of torque angle [29], MPC's cost function [30], and evaluating inverter switching statistics [15], [31] for ISCF detection.

Recently, the utilization of artificial intelligence (AI) techniques, such as neural networks (NN), has been gaining increasing momentum in power electronics [32], [33]. A particular area for which the NN approach is very suitable is the fault diagnosis of electrical machines. Several studies have developed AI-based fault detection methods as reviewed in [34]–[37]. They mostly use stator currents or vibration signals from additional sensors to extract the fault data.

While most of these studies are for bearing fault diagnosis [34], few are for ISCF [38]–[45]. Studies [38]–[41] use neural networks to detect ISCFs in permanent magnet synchronous machines (PMSMs). Convolutional neural networks using stator phase currents, voltages, or flux as input, for example, are utilized for ISCF detection in [38], which requires additional sensors. Similarly, an NN-based method detects ISCFs down to 4.2% using phase currents and speed information in a closed-loop controlled machine in [41]. However, no details regarding the controller structure or the controller-fault interaction are provided. For IMs, a data-driven online detection method utilizing multiple classifiers is proposed in [42]. The fault information is acquired from phase currents and voltages. ISCFs down to 2% could have been detected. A multi-layer perceptron is trained to detect ISCFs down to 0.6% in [43]. The three-phase shifts are utilized as the input data. An unsupervised learning-based NN using phase currents for fault detection is reported in [44]. Similarly, ISCF detection is achieved in [45] using an NN-based method on stator currents of an IM driven by an inverter via open-loop scalar *V/f* control. While these studies [42]–[45] consider IMs that work in an open-loop fashion, a closed-loop controlled IM, driven by a model predictive control structure is considered in this paper, which constitutes a fundamental difference.

The voltage vectors of a two-level voltage source inverter (2L-VSI) are depicted in Fig. 1a. In the standard FCS-MPC, the controller finds the optimum voltage vector in view of the control outcomes and applies it at the next switching instant. Hence, the controller outcomes are discrete voltage vectors and convenient for statistical approaches.

The evident benefits of achieving fault detection by examining controller outcomes are being non-invasive and requiring no additional sensor or circuit contrary to studies [25]–[27]. Hence, no extra cost or complexity is introduced since switching vectors produced by the controller are readily available for analysis.

To the authors' knowledge, the utilization of inverter switching statistics for ISCF diagnosis was first proposed by [31]. Later, it was utilized in [15] for ISCF detection in an IM driven by FCS-MPC using a simple thresholding-based approach with a manually set threshold level. This paper employs NNs for ISCF diagnosis using inverter switching vectors of the same experimental setup of [15]. With the utilization of NNs, improved fault detection performance over a broader range on the torque-speed plane is achieved in this study.

A motor drive inverter with model predictive control produces an (almost) uniform distribution of active switching vectors while driving a healthy induction machine. However, an inter-turn short circuit in the stator changes the distribution of active switching vectors since the driver tries to compensate for the fault's influence for the proper operation of the motor (Fig. 1b). This observation constitutes the basis for this study. Our primary approach is to train a neural network with the switching vector data collected for healthy and faulty cases so that the trained structure can identify and locate an ISCF. The detection performance results prove the effectiveness of the proposed approach.

There are three main contributions of this paper.

1) A machine learning-based, non-invasive ISCF detection method using inverter switching statistics is introduced.
2) The first publicly available ISCF detection dataset containing switching vector data collected at various load torque and shaft speed values for healthy and faulty states of an induction machine is released.

3) Performance baselines on the released dataset for three main neural network architectures, namely, multi-layer perceptron, convolutional neural network, and recurrent neural network are provided.

II. Neural Network Based ISCF Detection

This study designs neural network models detecting inter-turn short circuit faults in an induction machine driven by an inverter with model predictive control (Fig. 1c and Fig. 2). We formulate ISCF detection as a classification problem using inverter switching statistics.

A. Problem Formulation

Let $\boldsymbol{X} = \{\boldsymbol{x}_1, \cdots, \boldsymbol{x}_N\}$ be a set of training samples such that each sample $\boldsymbol{x}_i \in \mathbb{R}^D$ has a corresponding ground-truth label $\boldsymbol{y}_i = [y_i^1, \cdots, y_i^K] \in \{0,1\}^K$ where $\sum_{k=1}^K y_i^k = 1$. Given a model is represented as a function parameterized by θ, $f_\theta : \mathbb{R}^D \to \mathbb{R}^K$, it predicts the label of an input sample $\boldsymbol{x}_i$ as $\hat{\boldsymbol{y}}_i = f_\theta(\boldsymbol{x}_i) = [\hat{y}_i^1, \cdots, \hat{y}_i^K] \in \mathbb{R}^K$ such that $\hat{y}_i^k \geq 0 \; \forall k$ and $\sum_{k=1}^K \hat{y}_i^k = 1$. We train a model end-to-end using categorical-cross entropy as the loss function (1).

$$loss = \frac{1}{N} \sum_{i=1}^{N} \sum_{k=1}^{K} y_i^k \log \hat{y}_i^k \tag{1}$$

B. Neural Network Model Architectures

We constructed three different models using multi-layer perceptron (MLP), convolutional neural network (CNN), and recurrent neural network (RNN) architectures. Models are designed such that they have almost the same number of learnable parameters, i.e. 'capacity' (MLP: 4612, CNN: 4417, and RNN: 4418 learnable parameters). A model accepts a histogram of inverter switching statistics at the input and predicts the machine's status (healthy or faulty) at the output.

The multi-layer perceptron model consists of an input layer with 4 nodes, two hidden layers with 64 nodes, and an output layer with 2 nodes (Fig. 1c). Each layer computes a weighted sum of its inputs ($s_j = \sum_i w_{ji} x_i + b_j$, where $\mathbf{s} = [s_j]$ is the output vector, $\mathbf{x} = [x_i]$ is the input vector, $\mathbf{W} = [w_{ji}]$ is the learnable weight matrix, and $\mathbf{b} = [b_j]$ is the learnable bias vector), followed by a non-linear activation function. Hidden layers have a ReLU activation function ($f(s) = \max(0, s)$) followed by a dropout with a rate of 0.5. The output layer has a softmax activation function producing normalized probability values, i.e., adding up to 1.

The convolutional neural network model consists of three convolutional layers with 32, 64, and 2 filters, respectively (Fig. 2a). Each convolutional layer computes a cross-correlation of its inputs and filter weights ($s_j = \sum_i w_i x_{j+i} + b$, where $\mathbf{W} = [w_{ji}]$ is the learnable and shared filter weights and b is the learnable bias). Except the last layer, each convolutional layer is followed by a ReLU activation function and a dropout with a rate of 0.5. Similar to the MLP model, outputs at the last layer are normalized using a softmax activation function.

The recurrent neural network model consists of a recurrent cell containing 64 hidden nodes and a fully connected layer as a linear classifier on top (Fig. 2b). A recurrent cell computes an affine transformation of the input and the previous hidden state, adds them up and passes through a non-linear activation function to compute the current hidden state ($h_t = f(\mathbf{W}_{ih}\mathbf{x} + \mathbf{b}_{ih} + \mathbf{W}_{hh}\mathbf{h}_{t-1} + \mathbf{b}_{hh})$, where $\mathbf{W}_{ih}$ and $\mathbf{W}_{hh}$ are learnable weight matrices, and $\mathbf{b}_{ih}$ and $\mathbf{b}_{hh}$ are learnable bias vectors). Note that non-linear activation function is ReLU, and after each recurrent step a dropout with a rate of 0.5 is applied on hidden state.

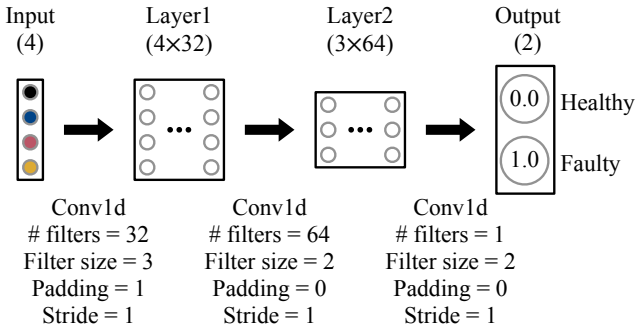

(a) Convolutional neural network.

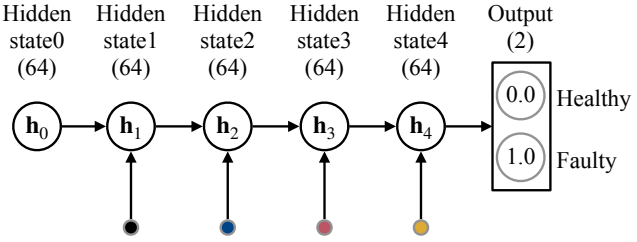

(b) Recurrent neural network.

Fig. 2: **Neural network models.**

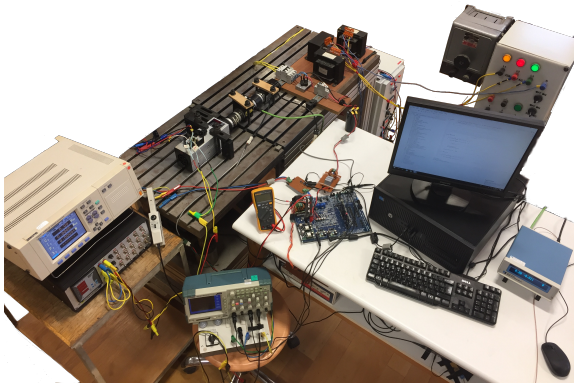

Fig. 3: **Experimental setup.** An FCS-MPC driven IM is used in the experiments. The ISCF condition corresponds to a short-circuiting of 2-turns out of 104-turns in a phase winding.

C. Experimental Setup and Preparation of the Machine Learning Dataset

The switching vectors of the motor drive inverter were collected from the same experimental setup utilized in [15]. A photo of the setup is provided in Fig. 3. The parameters of the IM, on which intentional ISCFs of 2, 3, and 5 turns can be created for tests, are given in Table I as utilized in the MPC

TABLE I: **Induction Machine (IM) parameters.**

Name	Symbol	Value
Apparent power	S	640 VA
Stator voltage	V_{ab}	128 V
Stator current	I	2.9 A
Base frequency	f	50 Hz
Torque	T_e	1.2 N.m
Number of poles	p	2
Total turns in one phase	N_s	104
Stator resistance	R_s	2.3 Ω
Rotor resistance	R_r	3.1 Ω
Magnetizing inductance	L_m	98 mH
Stator leakage inductance	L_{ls}	4 mH
Rotor leakage inductance	L_{lr}	2 mH
Stator flux magnitude reference	$\|\Psi_s\|^{ref}$	0.3 Wb

loop. The motor drive development kit TMDXIDDK379D from Texas Instruments is used as the motor drive inverter. The interested reader is referred to [46] for detailed descriptions regarding the FCS-MPC structure and equations, the laboratory implementation, and various test results including motor drive operation and the ISCF detection through switching vector analysis based on a simple thresholding method.

For several different combinations of speed and torque at healthy and faulty states (see Table II), the voltage vectors (decided by the controller and executed by the inverter) are recorded as time series of 22000 elements. The FCS-MPC algorithm has a control frequency of 40 kHz, therefore the record for the switching vector array of 22000 elements corresponds to a total of 0.55 second time interval. In the creation of Table II, frequency and torque values are read from the waveform analyzer and torque sensor respectively, which are involved in the experimental setup shown in Fig. 3. ISCFs were introduced over 2 out of 104 turns in a phase winding of a star connected IM. Short circuits were created over an external cable, which introduces an additional resistance of 0.13 Ω and no additional resistance was utilized to resemble the fault resistance. Experimental results depicting successful fault detection performance with the simple thresholding approach for additional external fault resistances of 0.2 Ω and 0.33 Ω are provided in [46].

Collected data series (healthy: 30, faulty: 34) were segregated into two sets such that the first set (healthy: 16, faulty: 18) was for training and validation, and the second set (healthy: 14, faulty: 16) was for the test. Each data series in the first set was further split into two. The first 70% of data points constituted a data series for training, and the remaining 30% constituted a data series for validation. Then, machine learning datasets of training, validation, and test were prepared by creating sample and label pairs over respective data series. The dataset details are available with the released code [47].

Over a data series, multiple samples were created in a sliding window fashion with a step size of one. A sample was created by calculating the histogram of switching vectors over a window of five electrical periods (≈ 92 ms at the rated speed and torque) (Fig. 1b). Note that switching vectors were aggregated as 0-vectors ($v_0 - v_7$), phase A vectors ($v_1 - v_4$), phase B vectors ($v_3 - v_6$), and phase C vectors ($v_2 - v_5$). The machine's status (i.e., healthy or faulty) was assigned as the sample's label.

TABLE II: **Data for ISCF detection.** Inverter switching vectors were collected for different conditions (H: healthy and F: faulty) of an induction machine with a rated speed of $w = 3000$ rpm and a rated torque of $T = 1.20$ N·m. The collected data series were segregated into two sets such that the first set (H:16, F:18) was for training and validation, and the second set (H:14, F:16) was for the test. Speed (w), torque (T), measured electrical frequency (f_e), and the number of healthy and faulty data series in the machine learning dataset are presented. Each data series in the first set was divided into two such that the first 70% and the remaining 30% were used to create samples for the training and validation sets, respectively. Data series in the second set were used to create samples for the test set.

w (rpm)	T (N·m)	f_e (Hz)	Training & Validation	Test
1500	0.30, 0.90	25.5, 28.0	H:2, F:2	H:2, F:2
2250	0.30, 1.25	38.1, 42.0	H:3, F:4	H:3, F:4
3000	0.30, 1.20, 1.30, 1.35	50.6, 54.4, 54.8, 55.3	H:4, F:4	H:4, F:4
3750	0.30, 1.25	63.1, 67.5	H:3, F:4	H:3, F:4
4500	0.30, 1.15	75.6, 79.8	H:4, F:4	H:2, F:2

D. Training and Testing of The NN Model

A neural network model was trained on samples created from training data series using the loss function given in Eq. 1. Early stopping based on loss in the validation dataset was employed to avoid overfitting. Finally, the model's performance was evaluated on the unseen test dataset. Please note that all models were trained and tested offline. They require neither storing the current dataset nor collecting new data during operation to identify ISCFs.

The area under the receiver operating characteristic curve (AUROC) was used as the performance metric. We also calculated the 95% confidence interval (CI) of the AUROC using the percentile bootstrap method [48].

E. Data and Code Availability

All original code and the dataset have been deposited at Zenodo under the https://doi.org/10.5281/zenodo.6774360 and made publicly available [47]. The dataset, code, and performance baselines are valuable resources to the research community for enabling reproducible and comparable experiments.

III. Results

A. The NNs Detect ISCF

We checked the performance of neural network models on ISCF detection. For each sample in the test set, we obtained a prediction from each trained model and plotted the receiver operating characteristic curves. We obtained AUROC values of 0.9946 (95% CI: 0.9945 - 0.9947), 0.9942 (95% CI: 0.9940 - 0.9943), and 0.9950 (95% CI: 0.9949 - 0.9951) for the MLP, CNN, and RNN models, respectively.

TABLE III: **ISCF detection performance comparison.** We compared our models' performances on ISCF detection task with the performances of the models in [38]. We also presented the type of neural network models, the number of learnable parameters in each model, input signals to the models, and the number of healthy and faulty samples in the test sets. If there is an extra sensor requirement for an input signal, it is also indicated.

Reference	NN type	# learnable parameters	Input signal	# samples in the test set	Accuracy
[38]	CNN	≈12,000	Stator phase currents	Healthy: 1,800 - Faulty: 5,400	0.9114
[38]	CNN	≈32,000	Stator phase-to-phase voltages (extra sensors)	Healthy: 1,800 - Faulty: 5,400	0.9501
[38]	CNN	≈6,000	Axial flux signal (extra sensor)	Healthy: 1,800 - Faulty: 5,400	0.9940
Ours	MLP	4,612	Inverter switching statistics	Healthy: 248,844 - Faulty: 284,466	0.9632
Ours	CNN	4,417	Inverter switching statistics	Healthy: 248,844 - Faulty: 284,466	0.9634
Ours	RNN	4,418	Inverter switching statistics	Healthy: 248,844 - Faulty: 284,466	0.9611

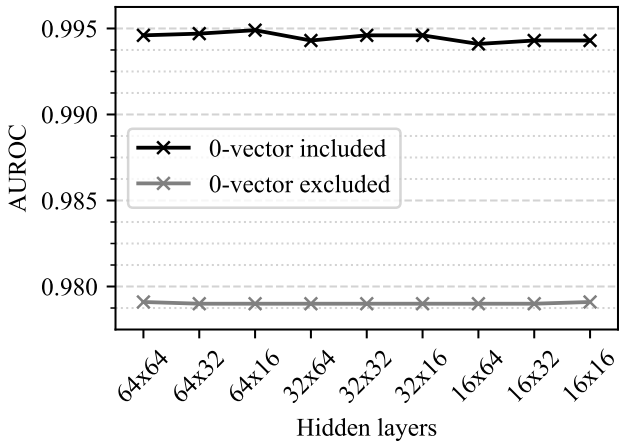

Fig. 4: **The neural network models detect ISCF.** Different NN models using the same architecture with different number of nodes in the hidden layers were trained and tested on the ISCF detection task. The area under receiver operating characteristics curve (AUROC) calculated on the test set was used as performance metric. We trained and tested the models using histogram of all vectors (0-vector included) and active vectors only (0-vector excluded).

We also compared our models' performances with the performances of the models in [38] (Table III). Our models were about 1.3 to 7 times smaller, and our test set was about 74 times bigger than the models and test set in [38], respectively. Our models performed better than the models of [38] using stator currents and voltages. On the other hand, the model using the axial flux signal in [38] had a better performance than ours. However, it required an additional sensor for flux measurements, which was not the case for our models.

To check our models' generalization ability, we excluded data series collected at $w = 2250$ rpm and $w = 3750$ rpm from the training set (Table II). We retrained our MLP model from scratch. Similar to the performance of our MLP model trained on the whole training set, an AUROC value of 0.9946 (95% CI: 0.9945 - 0.9947) was obtained on the test set. Furthermore, the model achieved an AUROC value of 0.9998 (95% CI: 0.9998 - 0.9998) on data series collected at $w = 2250$ rpm and $w = 3750$ rpm in the test set (Table II), showing our model's generalization ability. Please note that the model had never seen data from a data series at these speeds.

We also analyzed the effect of training set size on the model's performance. We excluded some of the data series having similar speed and torque values from the training set (i.e., data series 6, 8, 11, 13, 15, 21, 23, 26, 28, 30, 32, and 34 were excluded (Table II)). Our MLP model was retrained from scratch and tested on the test set. Although the model was trained on less than 65% of the original training set, it achieved an AUROC value of 0.9944 (95% CI: 0.9943 - 0.9945) on the test set, which was similar to the performance of the model trained on the whole training set.

To determine the MLP model's architecture, we conducted a hyperparameter search on hidden-layer sizes in the MLP model. By varying the hidden layer sizes (16, 32, or 64 nodes in each hidden layer), we analyzed the effect of the model's capacity on its performance. As expected, we observed that the model's performance decreased with decreasing model capacity (Fig. 4). Therefore, we performed our experiments using the MLP model with 64 nodes in its two hidden layers. Nevertheless, the performance decrease was not drastic in the smaller networks, which could be preferable for real-world deployment since they require less computational power.

Besides, we checked the model's performance on identifying if a data series was collected at the healthy or faulty state of the machine. Prediction for a data series was obtained as the average of predictions of all samples created from the data series. Although we observed wrong predictions at the sample level in the few data series, the model *perfectly* identified the machine's status at the data series level (Fig. 5).

B. 0-vectors Help The NN Detect ISCF

We know that the proportion of 0-vectors provides information about the speed and torque of the machine, which can be valuable for the model. To test the effect of 0-vectors on the performance of the neural network model, we excluded 0-vectors from histogram calculation and reran our experiments. As expected, we observed a performance decrease (Fig. 4). Hence, we concluded that 0-vectors helped the neural network models detect ISCF.

Furthermore, we observed a decrease in fault detection performance for the speed values beyond 3750 rpm (Fig. 5). This region corresponds to the verge of overmodulation in an inverter control system with a carrier-based modulation, where the percentage of zero vectors significantly decreases. The switching vector statistics were also not as responsive to the occurrence of the fault as they were at the slower speeds.

This article has been accepted for publication in IEEE Transactions on Energy Conversion. This is the author's version which has not been fully edited and content may change prior to final publication. Citation information: DOI 10.1109/TEC.2023.3274052

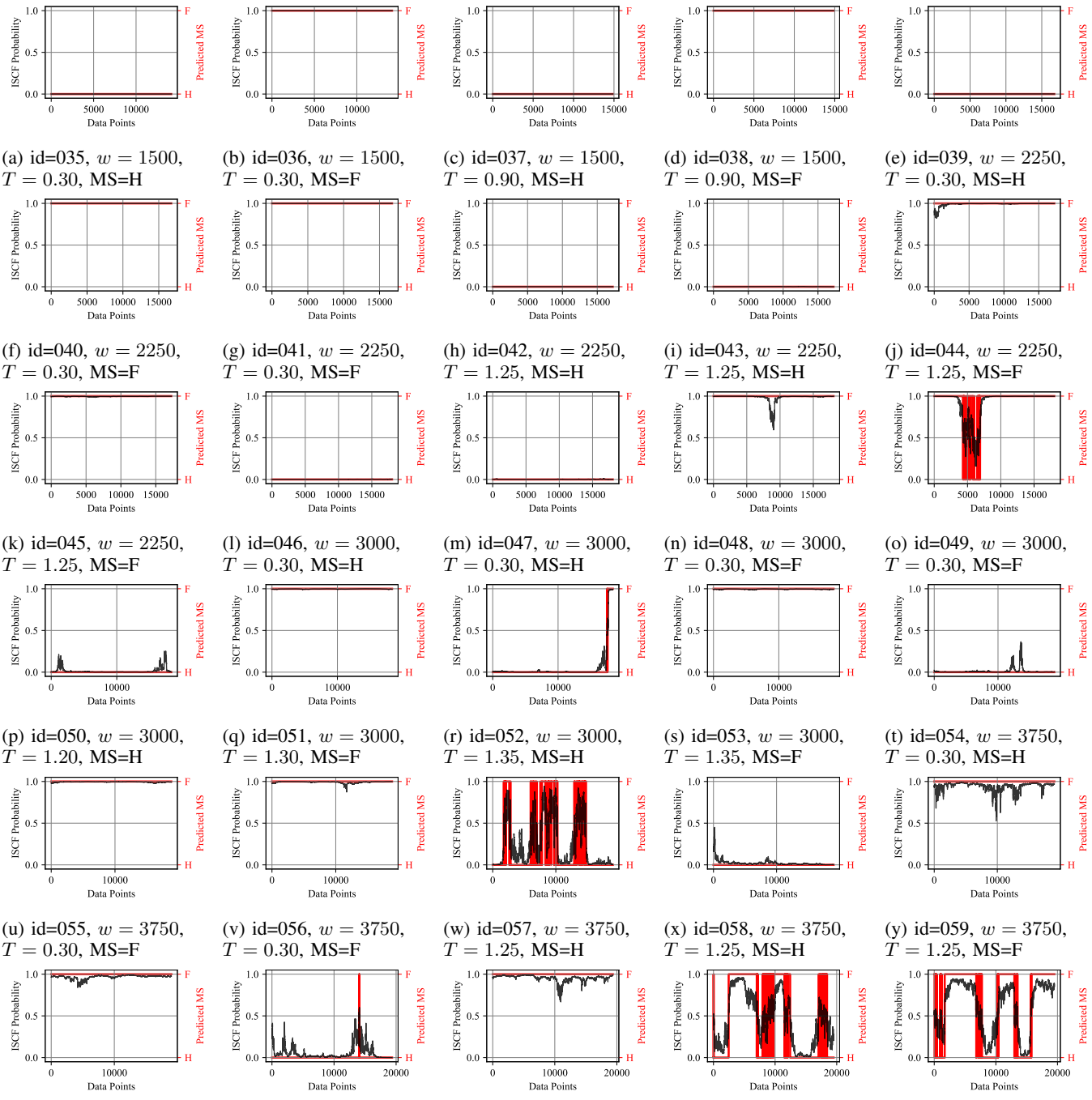

(a) id=035, $w = 1500$, $T = 0.30$, MS=H
(b) id=036, $w = 1500$, $T = 0.30$, MS=F
(c) id=037, $w = 1500$, $T = 0.90$, MS=H
(d) id=038, $w = 1500$, $T = 0.90$, MS=F
(e) id=039, $w = 2250$, $T = 0.30$, MS=H
(f) id=040, $w = 2250$, $T = 0.30$, MS=F
(g) id=041, $w = 2250$, $T = 0.30$, MS=F
(h) id=042, $w = 2250$, $T = 1.25$, MS=H
(i) id=043, $w = 2250$, $T = 1.25$, MS=H
(j) id=044, $w = 2250$, $T = 1.25$, MS=F
(k) id=045, $w = 2250$, $T = 1.25$, MS=F
(l) id=046, $w = 3000$, $T = 0.30$, MS=H
(m) id=047, $w = 3000$, $T = 0.30$, MS=H
(n) id=048, $w = 3000$, $T = 0.30$, MS=F
(o) id=049, $w = 3000$, $T = 0.30$, MS=F
(p) id=050, $w = 3000$, $T = 1.20$, MS=H
(q) id=051, $w = 3000$, $T = 1.30$, MS=F
(r) id=052, $w = 3000$, $T = 1.35$, MS=H
(s) id=053, $w = 3000$, $T = 1.35$, MS=F
(t) id=054, $w = 3750$, $T = 0.30$, MS=H
(u) id=055, $w = 3750$, $T = 0.30$, MS=F
(v) id=056, $w = 3750$, $T = 0.30$, MS=F
(w) id=057, $w = 3750$, $T = 1.25$, MS=H
(x) id=058, $w = 3750$, $T = 1.25$, MS=H
(y) id=059, $w = 3750$, $T = 1.25$, MS=F
(z) id=060, $w = 3750$, $T = 1.25$, MS=F
(aa) id=061, $w = 4500$, $T = 0.30$, MS=H
(ab) id=062, $w = 4500$, $T = 0.30$, MS=F
(ac) id=063, $w = 4500$, $T = 1.15$, MS=H
(ad) id=064, $w = 4500$, $T = 1.15$, MS=F

Fig. 5: **Sample-level ISCF predictions on the data series in the test dataset.** At each point of a data series (i.e., for a sample), inter-turn short circuit fault (ISCF) probability was obtained from the trained model. ISCF probability and predicted machine status (MS) obtained by thresholding the predicted probability value with 0.5 are presented for data series. For each data series, id, speed (rpm), torque (N·m), and MS ((H)ealthy, (F)aulty) are also given.

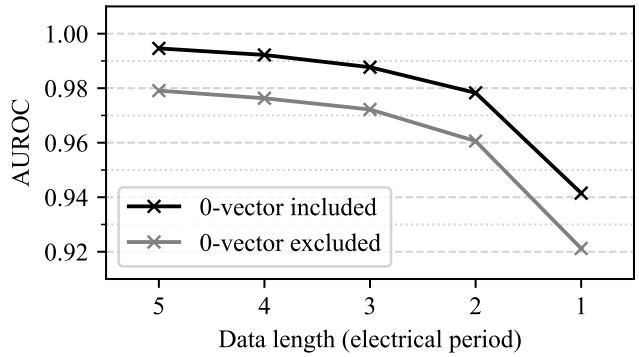

Fig. 6: **Statistics over longer intervals improve performance.** Switching vector histograms were calculated over an interval of multiples of electrical period (5,4,3,2, and 1) while training the NN models. We compared the effect of interval length on the model's performance using AUROC on the test set both for 0-vector included and 0-vector excluded cases.

C. Statistics Over Longer Intervals Improve Performance

We trained and tested our models with sample and label pairs. A sample was created by calculating the histogram of switching vectors over a window of five electrical periods ($\approx$ 92 ms at the rated speed and torque). In an ideal system (where there is no noise), an ISCF can be detected using inverter switching statistics calculated over one electrical period. However, the system is noisy in practice, and the noise directly affects the model's performance.

We investigated the effects of the interval length, over which switching vector histograms were calculated, on the performance of neural network models. We observed that as the length of the interval decreased (multiples of electrical period: 5, 4, 3, 2, and 1), the model's performance also decreased (Fig. 6). In short, we concluded that statistics over longer intervals improved the model's performance.

One interesting observation was that the performance decay was gradual from five to two periods. Nevertheless, it was drastic from two periods to a single period. Our observation was also consistent with the findings of [15], which uses a thresholding-based method over switching vector statistics. Besides, the contribution of 0-vectors in the model's performance was evident (Fig. 6).

D. The NN Identifies Faulty Phase in a Machine with ISCF

After we showed that a neural network model successfully detected ISCF, we also checked if it could identify the faulty phase. We prepared a small dataset using data series collected at the rated speed ($w = 3000$ rpm) and around the rated torque ($T = 1.20$ N·m) of the induction machine.

Training, validation, and test sets were prepared similar to the previous data segregation. Two healthy and three faulty (one for each phase) data series were used for preparing data samples in each set. The dataset details are available with the released code [47].

We modified the neural network architecture used in ISCF detection to a multi-class classification model with four classes corresponding to the machine's status of healthy, faulty (A), faulty (B), and faulty (C). Then, we trained the model on the training set with early stopping based on loss in the validation set and evaluated its performance on the test set. The model successfully detected ISCF and identified the faulty phase (Table IV). It achieved an accuracy of 0.9995. As in the ISCF detection task, our neural network model perfectly detected ISCF and identified the faulty phase at the data series level.

TABLE IV: **Faulty phase detection.** The same NN architecture was modified to a multi-class classification model detecting faulty phase as well. The confusion matrix obtained on the test set is presented.

		Predicted			
		Healthy	Faulty (A)	Faulty (B)	Faulty (C)
Truth	Healthy	1.000	0.000	0.000	0.000
	Faulty (A)	0.000	1.000	0.000	0.000
	Faulty (B)	0.000	0.000	1.000	0.000
	Faulty (C)	0.003	0.000	0.000	0.997

E. The NN Outperforms Thresholding Based Method

The duration of high electrical currents passing through the shorted turns during an ISCF is critical for the repair and possible fault-tolerant operation of the machine. As the detection time takes longer, the ISCF condition will evolve further into the unmanageable situations such as complete phase to phase or phase to ground shorts. Therefore, we compared the performance of our neural network model with the thresholding-based method of [15] in terms of ISCF detection time. At various load torque and shaft speed values, while the thresholding-based method detected ISCF in between 0.5 to 2 seconds, the neural network model detected ISCF in between 0.074 to 0.196 seconds. There was a speedup of more than two times at the rated operating conditions (≈ 0.2 second for the thresholding-based method in [46] and 0.092 seconds for our neural network model).

IV. Conclusion

Early detection of an ISCF in an electrical machine is vital for its maintenance. This study developed neural network models that detect an ISCF in an IM driven by an inverter with an MPC algorithm. The models accepted the histogram of inverter switching vectors, which are readily available, as input and predicted the machine's status (healthy or faulty) at the output (Fig. 1). An ISCF in the IM was successfully detected under 0.1 seconds with an almost perfect performance (Fig. 4). Besides, the faulty phase was identified with an accuracy of 0.9995 (Table IV).

In our experiments, while the large networks performed slightly better in the ISCF detection task, the performance of the smaller networks were also good enough for real-world deployment (Fig. 4). Moreover, a small network requires less memory and computational resources, facilitating its deployment in the same processor alongside the controller algorithm.

Our experiments validated that 0-vectors contained valuable information for ISCF detection (Fig. 4), and statistics over

longer intervals improved the performance (Fig. 6). Nevertheless, there was a trade-off between better performance and faster ISCF detection in determining the optimum interval for statistics calculation. We concluded that an interval of three to five electrical periods was reasonable.

Lastly, the proposed approach evaluates the inverter switching vectors that are already available as controller outputs, i.e., it is non-invasive. Besides, different than some online signal-processing-based techniques requiring extra sensors [25]–[27], our method does not require any extra sensors. Hence, no significant cost or complexity is introduced.

A. Limitations and Future Work

To avoid data leakage in our experiments, we used data series collected at different runs in training and test sets (Table II), i.e., we tested the models on unseen data [49]. Besides, our model successfully detected ISCFs in data series collected at speed and torque values that were different from the speed and torque values of the data series in the model's training set, showing our model's generalization ability. Our model could perform quite well for machines of the same manufacturer with similar specifications. However, it might require fine-tuning for machines of different manufacturers or specifications, known as domain adaptation and a hot topic in machine learning research [50], [51]. Therefore, it would have been better to test the trained model on data from another machine, which we have kept as future work.

Furthermore, we observed that the model's performance started to degrade beyond the rated speed and torque values (Fig. 5), which corresponds to the operation on the verge of overmodulation, where the utilization of zero vectors significantly decreases. This could be due to the limited available data around these operation regions of the IM. We had around 300k samples in our training set; however, they were created from only 26 independent data series (Table II). Since data collection is quite expensive, our dataset was minimal compared to traditional deep learning datasets containing millions of independent samples [52]. Besides, all healthy data points in our dataset were collected in a short period of time relative to lifetime of a machine, so our dataset did not capture the aging effects, such as the change of motor parameters or insulator degradation over time. Hence, the collection of an extensive dataset and the real-world deployment of our ISCF detection models are reserved for future work. The prospective dataset should broadly cover the IM's operation regions, including different operating scenarios, temperatures, and DC-bus voltages, over a sufficiently long time interval to include the aging effects.

Lastly, this study focused on detecting ISCF of $\sim$2% of turns (2 out of 104). It did not consider severe cases, like ISCFs of high percentages or phase-to-phase and phase-to-ground short circuits. Nevertheless, their effects on the input variables would be more evident, and NNs would have easily identified them. Similarly, this study did not consider rotor and bearing faults. Although controller-fault interactions would be anticipated for the rotor and bearing faults, an ISCF can be discriminated from these fault types by their characteristics. A rotor fault's influence would be effective on each phase equally, and the bearing fault's rate of progression would be considerably slower compared to the ISCF case. In addition to detecting a fault independent of the inflicting fault type, identification of fault type would be valuable. Hence, preparing an extensive dataset including different fault types and operating scenarios is essential in future work.

ACKNOWLEDGMENTS

We thank Öztürk Şahin Alemdar for constructive comments.

REFERENCES

[1] S. Nandi, H. Toliyat, and X. Li, "Condition monitoring and fault diagnosis of electrical motors—a review," *IEEE Transactions on Energy Conversion*, vol. 20, no. 4, pp. 719–729, 2005.

[2] H. Henao, G.-A. Capolino, M. Fernandez-Cabanas, F. Filippetti, C. Bruzzese, E. Strangas, R. Pusca, J. Estima, M. Riera-Guasp, and S. Hedayati-Kia, "Trends in fault diagnosis for electrical machines: A review of diagnostic techniques," *IEEE Industrial Electronics Magazine*, vol. 8, no. 2, pp. 31–42, 2014.

[3] A. Gandhi, T. Corrigan, and L. Parsa, "Recent advances in modeling and online detection of stator interturn faults in electrical motors," *IEEE Transactions on Industrial Electronics*, vol. 58, no. 5, pp. 1564–1575, 2011.

[4] Y. Chen, S. Liang, W. Li, H. Liang, and C. Wang, "Faults and diagnosis methods of permanent magnet synchronous motors: A review," *Applied Sciences*, vol. 9, no. 10, p. 2116, 2019.

[5] A. Bellini, F. Filippetti, C. Tassoni, and G.-A. Capolino, "Advances in diagnostic techniques for induction machines," *IEEE Transactions on Industrial Electronics*, vol. 55, no. 12, pp. 4109–4126, 2008.

[6] A. Siddique, G. Yadava, and B. Singh, "A review of stator fault monitoring techniques of induction motors," *IEEE Transactions on Energy Conversion*, vol. 20, no. 1, pp. 106–114, 2005.

[7] R. T. Purushottam Gangsar, "Signal based condition monitoring techniques for fault detection and diagnosis of induction motors: A state-of-the-art review," *Mechanical Systems and Signal Processing*, vol. 144, 2020.

[8] A. H. Bonnett and C. Yung, "Increased efficiency versus increased reliability," *IEEE Industry Applications Magazine*, vol. 14, no. 1, pp. 29–36, 2008.

[9] A. Bonnett and G. Soukup, "Cause and analysis of stator and rotor failures in three-phase squirrel-cage induction motors," *IEEE Transactions on Industry Applications*, vol. 28, no. 4, pp. 921–937, 1992.

[10] C. Gerada, K. Bradley, M. Sumner, P. Wheeler, S. Picker, J. Clare, C. Whitley, and G. Towers, "The results do mesh," *IEEE Industry Applications Magazine*, vol. 13, no. 2, pp. 62–72, 2007.

[11] S. Cheng, P. Zhang, and T. G. Habetler, "An impedance identification approach to sensitive detection and location of stator turn-to-turn faults in a closed-loop multiple-motor drive," *IEEE Transactions on Industrial Electronics*, vol. 58, no. 5, pp. 1545–1554, 2011.

[12] M. Zafarani, E. Bostanci, Y. Qi, T. Goktas, and B. Akin, "Interturn short-circuit faults in permanent magnet synchronous machines: An extended review and comprehensive analysis," *IEEE Journal of Emerging and Selected Topics in Power Electronics*, vol. 6, no. 4, pp. 2173–2191, 2018.

[13] T. Orlowska-Kowalska, M. Wolkiewicz, P. Pietrzak, M. Skowron, P. Ewert, G. Tarchala, M. Krzysztofiak, and C. T. Kowalski, "Fault diagnosis and fault-tolerant control of pmsm drives–state of the art and future challenges," *IEEE Access*, vol. 10, pp. 59 979–60 024, 2022.

[14] K.-H. Kim, D.-U. Choi, B.-G. Gu, and I.-S. Jung, "Fault model and performance evaluation of an inverter-fed permanent magnet synchronous motor under winding shorted turn and inverter switch open," *IET Electr. Power Appl.*, vol. 4, no. 4, pp. 214–225, 2010.

[15] İ. Şahin and O. Keysan, "Model predictive controller utilized as an observer for inter-turn short circuit detection in induction motors," *IEEE Transactions on Energy Conversion*, vol. 36, no. 2, pp. 1449–1458, 2021.

[16] J. Hang, Q. Hu, W. Sun, X. Ren, S. Ding, Y. Huang, and W. Hua, "A voltage-distortion-based method for robust detection and location of interturn fault in permanent magnet synchronous machine," *IEEE Transactions on Power Electronics*, vol. 37, no. 9, pp. 11 174–11 186, 2022.

[17] Y. Xu, Y. Wang, and J. Zou, "An inter-turn short-circuits fault detection strategy considering inverter nonlinearity and current measurement errors for sensorless control of spmsm," *IEEE Transactions on Industrial Electronics*, vol. 69, no. 11, pp. 11 709–11 722, 2022.

[18] A. Mahmoudi, I. Jlassi, A. J. M. Cardoso, K. Yahia, and M. Sahraoui, "Inter-turn short-circuit faults diagnosis in synchronous reluctance machines, using the luenberger state observer and current's second-order harmonic," *IEEE Transactions on Industrial Electronics*, vol. 69, no. 8, pp. 8420–8429, 2022.

[19] M. Wolkiewicz, G. Tarchała, T. Orłowska-Kowalska, and C. T. Kowalski, "Online stator interturn short circuits monitoring in the dfoc induction-motor drive," *IEEE Transactions on Industrial Electronics*, vol. 63, no. 4, pp. 2517–2528, 2016.

[20] K.-H. Kim, "Simple online fault detecting scheme for short-circuited turn in a pmsm through current harmonic monitoring," *IEEE Transactions on Industrial Electronics*, vol. 58, no. 6, pp. 2565–2568, 2011.

[21] J. A. Rosero, L. Romeral, J. A. Ortega, and E. Rosero, "Short-circuit detection by means of empirical mode decomposition and wigner–ville distribution for pmsm running under dynamic condition," *IEEE Transactions on Industrial Electronics*, vol. 56, no. 11, pp. 4534–4547, 2009.

[22] J. Bonet-Jara, J. Pons-Llinares, and K. N. Gyftakis, "Comprehensive analysis of principal slot harmonics as reliable indicators for early detection of inter-turn faults in induction motors of deep-well submersible pumps," *IEEE Transactions on Industrial Electronics*, vol. Early Access, pp. 1–11, 2022.

[23] S. Cruz and A. Cardoso, "Diagnosis of stator inter-turn short circuits in dtc induction motor drives," *IEEE Transactions on Industry Applications*, vol. 40, no. 5, pp. 1349–1360, 2004.

[24] M. Drif and A. J. M. Cardoso, "Stator fault diagnostics in squirrel cage three-phase induction motor drives using the instantaneous active and reactive power signature analyses," *IEEE Transactions on Industrial Informatics*, vol. 10, no. 2, pp. 1348–1360, 2014.

[25] H. H. Eldeeb, A. Berzoy, and O. Mohammed, "Stator fault detection on dtc-driven im via magnetic signatures aided by 2-d fea co-simulation," *IEEE Transactions on Magnetics*, vol. 55, no. 6, pp. 1–5, 2019.

[26] B. Wang, J. Hu, G. Wang, and W. Hua, "A novel stator turn fault detection technique by using equivalent high frequency impedance," *IEEE Access*, vol. 8, pp. 130 540–130 550, 2020.

[27] B. Sen and J. Wang, "Stator interturn fault detection in permanent-magnet machines using pwm ripple current measurement," *IEEE Transactions on Industrial Electronics*, vol. 63, no. 5, pp. 3148–3157, 2016.

[28] M. A. Mazzoletti, G. R. Bossio, C. H. De Angelo, and D. R. Espinoza-Trejo, "A model-based strategy for interturn short-circuit fault diagnosis in pmsm," *IEEE Transactions on Industrial Electronics*, vol. 64, no. 9, pp. 7218–7228, 2017.

[29] Z. Ullah, S.-T. Lee, and J. Hur, "A torque angle-based fault detection and identification technique for ipmsm," *IEEE Transactions on Industry Applications*, vol. 56, no. 1, pp. 170–182, 2020.

[30] J. Hang, J. Zhang, M. Xia, S. Ding, and W. Hua, "Interturn fault diagnosis for model-predictive-controlled-pmsm based on cost function and wavelet transform," *IEEE Transactions on Power Electronics*, vol. 35, no. 6, pp. 6405–6418, 2020.

[31] T. Wolbank, K. Loparo, and R. Wohrnschimmel, "Inverter statistics for online detection of stator asymmetries in inverter-fed induction motors," *IEEE Transactions on Industry Applications*, vol. 39, no. 4, pp. 1102–1108, 2003.

[32] B. K. Bose, "Artificial intelligence techniques: How can it solve problems in power electronics?: An advancing frontier," *IEEE Power Electronics Magazine*, vol. 7, no. 4, pp. 19–27, 2020.

[33] S. Zhao, F. Blaabjerg, and H. Wang, "An overview of artificial intelligence applications for power electronics," *IEEE Transactions on Power Electronics*, vol. 36, no. 4, pp. 4633–4658, 2021.

[34] S. Zhang, S. Zhang, B. Wang, and T. G. Habetler, "Deep learning algorithms for bearing fault diagnostics—a comprehensive review," *IEEE Access*, vol. 8, pp. 29 857–29 881, 2020.

[35] M. Seera, C. P. Lim, S. Nahavandi, and C. K. Loo, "Condition monitoring of induction motors: A review and an application of an ensemble of hybrid intelligent models," *Expert Systems with Applications*, vol. 41, no. 10, pp. 4891–4903, 2014.

[36] W. Lang, Y. Hu, C. Gong, X. Zhang, H. Xu, and J. Deng, "Artificial intelligence-based technique for fault detection and diagnosis of ev motors: A review," *IEEE Transactions on Transportation Electrification*, pp. 1–1, 2021.

[37] L. Wen, X. Li, L. Gao, and Y. Zhang, "A new convolutional neural network-based data-driven fault diagnosis method," *IEEE Transactions on Industrial Electronics*, vol. 65, no. 7, pp. 5990–5998, 2018.

[38] M. Skowron, T. Orlowska-Kowalska, and C. T. Kowalski, "Application of simplified convolutional neural networks for initial stator winding fault detection of the pmsm drive using different raw signal data," *IET Electric Power Applications*, vol. 15, no. 7, pp. 932–946, 2021.

[39] L. S. Maraaba, A. S. Milhem, I. A. Nemer, H. Al-Duwaish, and M. A. Abido, "Convolutional neural network-based inter-turn fault diagnosis in lspmsms," *IEEE Access*, vol. 8, pp. 81 960–81 970, 2020.

[40] H. Lee, H. Jeong, and S. W. Kim, "Detection of interturn short-circuit fault and demagnetization fault in ipmsm by 1-d convolutional neural network," in *2019 IEEE PES Asia-Pacific Power and Energy Engineering Conference (APPEEC)*. IEEE, 2019, pp. 1–5.

[41] H. Lee, H. Jeong, G. Koo, J. Ban, and S. W. Kim, "Attention recurrent neural network-based severity estimation method for interturn short-circuit fault in permanent magnet synchronous machines," *IEEE Transactions on Industrial Electronics*, vol. 68, no. 4, pp. 3445–3453, 2021.

[42] Z. Xu, C. Hu, F. Yang, S.-H. Kuo, C.-K. Goh, A. Gupta, and S. Nadarajan, "Data-driven inter-turn short circuit fault detection in induction machines," *IEEE Access*, vol. 5, pp. 25 055–25 068, 2017.

[43] M. B. K. Bouzid, G. Champenois, N. M. Bellaaj, L. Signac, and K. Jelassi, "An effective neural approach for the automatic location of stator interturn faults in induction motor," *IEEE Transactions on Industrial Electronics*, vol. 55, no. 12, pp. 4277–4289, 2008.

[44] J. F. Martins, V. Ferno Pires, and A. J. Pires, "Unsupervised neural-network-based algorithm for an on-line diagnosis of three-phase induction motor stator fault," *IEEE Transactions on Industrial Electronics*, vol. 54, no. 1, pp. 259–264, 2007.

[45] M. Skowron, T. Orlowska-Kowalska, M. Wolkiewicz, and C. T. Kowalski, "Convolutional neural network-based stator current data-driven incipient stator fault diagnosis of inverter-fed induction motor," *Energies*, vol. 13, no. 6, p. 1475, 2020.

[46] İ. Şahin, "Model predictive torque control of an induction motor enhanced with an inter-turn short circuit fault detection feature," Ph.D. dissertation, Middle East Technical University, 2021.

[47] M. Ümit Öner, İlker Şahin, and O. Keysan, "Inter-turn short circuit fault (iscf) detection," Jun. 2022. [Online]. Available: https://doi.org/10.5281/zenodo.6774360

[48] B. Efron, "Bootstrap methods: another look at the jackknife," in *Breakthroughs in statistics*. Springer, 1992, pp. 569–593.

[49] S. Kaufman, S. Rosset, C. Perlich, and O. Stitelman, "Leakage in data mining: Formulation, detection, and avoidance," *ACM Transactions on Knowledge Discovery from Data (TKDD)*, vol. 6, no. 4, pp. 1–21, 2012.

[50] M. Wang and W. Deng, "Deep visual domain adaptation: A survey," *Neurocomputing*, vol. 312, pp. 135–153, 2018.

[51] K. You, M. Long, Z. Cao, J. Wang, and M. I. Jordan, "Universal domain adaptation," in *Proceedings of the IEEE/CVF conference on computer vision and pattern recognition*, 2019, pp. 2720–2729.

[52] J. Deng, W. Dong, R. Socher, L.-J. Li, K. Li, and L. Fei-Fei, "Imagenet: A large-scale hierarchical image database," in *2009 IEEE Conference on Computer Vision and Pattern Recognition*, 2009, pp. 248–255.

Mustafa Umit Oner got his B.S. degree in 2013 and M.S. degree in 2016 from the Electrical and Electronics Engineering Department at the Middle East Technical University, Ankara, Turkiye. Then, he got his Ph.D. degree in 2021 from the Computer Science Department at the National University of Singapore, Singapore. He is currently an Assistant Professor at the Bahcesehir University, Istanbul, Turkiye. He is interested in developing novel machine learning models and machine learning-based information systems for digital histopathology and integrative multi-omics to support diagnostic and therapeutic decision-making in cancer.

İlker Şahin (Member, IEEE) received the B.Sc., M.Sc., and Ph.D. degrees in electrical and electronics engineering, in 2010, 2014, and 2021 respectively, from Middle East Technical University (METU), Ankara, Turkiye. From 2011 to 2020, he was a Teaching Assistant with METU, then he joined Aselsan in 2020, where he is currently working as a Lead Engineer. He was with the Institute for Energy Systems, School of Engineering, University of Edinburgh, as a post-doctoral researcher between May 2022 - March 2023. His current research interests include high-performance motor drives, predictive control, and fault diagnosis.

Ozan Keysan (Member, IEEE) received the master's degree from Middle East Technical University (METU), Ankara, Turkiye, in 2008, and the Ph.D. degree from the University of Edinburgh, Edinburgh, Scotland, in 2014. He is currently an Associate Professor with the Electrical and Electronics Engineering Department, METU. His current research interests include renewable energy, design, and optimization of electrical machines, smart grids, superconducting machines, and permanent-magnet machines.